Catalysis Today 142 (2009) 170–174

Contents lists available at ScienceDirect

Catalysis Today

journal homepage: www.elsevier.com/locate/cattod

The role of V in rutile-type Sn/V/Nb/Sb mixed oxides, catalysts for propane ammoxidation to acrylonitrile

Nicola Ballarini [a], Fabrizio Cavani [a,*], Philippe Marion [b], Nicandro Tonielli [a], Ferruccio Trifirò [a]

[a] Dipartimento di Chimica Industriale e dei Materiali, Università di, Bologna, Viale Risorgimento 4, 40136 Bologna, Italy
[b] Rhodia Operations, Centre de Recherches et Technologies, 85, Rue des Frères Perret, 69190 Saint Fons, France

ARTICLE INFO

Article history:
Available online 7 September 2008

Keywords:
Propane ammoxidation
Tin/vanadium/niobium/antimony oxide
Acrylonitrile
Rutile mixed oxides
Vanadium oxide

ABSTRACT

Rutile-type Sn/V/Nb/Sb mixed oxides of composition Sn/V/Nb/Sb 1/*x*/1/3 (atomic ratios) were prepared by co-precipitation from an alcoholic medium, characterized and tested as catalysts for the ammoxidation of propane to acrylonitrile. Vanadium had a relevant effect on chemical–physical and reactivity properties of catalysts. The latter consisted of Sn oxide incorporating Sb and Nb cations, of defective rutile-type V/Nb/Sb mixed oxide and of Sb oxide. Increasing amounts of V in samples caused an increase of the crystallinity and a corresponding decrease of the specific surface area. However, a relevant enhancement of the catalyst activity (rate of propane conversion per unit surface area) was observed. This was attributed to the generation of cationic vacancies, formed in the rutile-type V/Nb/Sb mixed oxide, that enhanced the intrinsic activity of V ions in the activation of the alkane. On the other hand, the selectivity to acrylonitrile declined considerably when the content of V in samples was increased, whereas the selectivity to carbon monoxide and that to cyanhydric acid increased.

1. Introduction

The ammoxidation of propane is currently investigated as a possible alternative to propene ammoxidation for acrylonitrile synthesis [1–5]. Different types of catalytic systems have been described in the literature for this reaction: (a) multicomponent rutile-type V-antimonates (e.g., V/Sb/W/Al/O) [3,4], (b) monophasic multicomponent molybdates (Mo/V/Nb/Te(Sb)/O) [6], and (c) V/Al mixed oxynitrides [7,8]. Multimetal molybdates, developed by Mitsubishi Kasei, give the highest yield to acrylonitrile under propane-lean conditions.

Rutile-type mixed oxides may contain several elements, each one playing a different role in the transformation of the alkane [9–11]. In regard to this, the rutile structure possesses the flexibility required to accommodate various elements in its framework. In previous works [12–14], we described the role of Sb and Nb, components of rutile-type Sn/V/Nb/Sb mixed oxides prepared by co-precipitation of the corresponding metal oxo-hydrates from an alcoholic solution. The thermal treatment of the precipitate led to the development of rutile compounds having coherent crystalline domains smaller than 10 nm, as inferred from X-ray diffraction patterns, that if compared with the more crystalline rutile systems prepared with the conventional "slurry" method are characterized by a greater structural defectivity, a higher specific surface area and a higher catalytic activity in propane ammoxidation. In the present paper, we report on the role of V in Sn/V/Nb/Sb/O systems.

2. Experimental

Catalysts were prepared using the co-precipitation technique, developed for the synthesis of rutile SnO_2-based systems claimed by Rhodia [12]. The preparation involved the dissolution of $SnCl_4{\cdot}5H_2O$, $VO(acac)_2$, $SbCl_5$ and $NbCl_5$ in absolute ethanol, and dropping the solution into buffered (pH 7) water. The precipitate obtained was separated from the supernatant liquid by filtration. The solid was then dried at 120 °C, and calcined in air at 700 °C for 3 h.

The XRD patterns of the catalysts were obtained with a Ni-filtered CuKα radiation on a Philips X'Pert vertical diffractometer equipped with a pulse height analyzer and a secondary curved graphite–crystal monochromator. Laser–Raman spectra were obtained using a Renishaw 1000 instrument; the samples were excited with the 514 nm Ar line. Specific surface areas were measured with the BET single-point method (Thermo Instrument).

Catalytic tests were carried out in a laboratory glass fixed-bed reactor at atmospheric pressure. 1.8 g of catalyst was loaded,

* Corresponding author.
E-mail address: fabrizio.cavani@unibo.it (F. Cavani).

0920-5861/$ – see front matter © 2008 Elsevier B.V. All rights reserved.
doi:10.1016/j.cattod.2008.07.033

shaped into particles with size from 0.42 mm to 0.55 mm. The following reaction conditions were used: (a) propane-rich feed: inlet composition 25 mol.% propane, 10% ammonia, 20% oxygen, remainder helium; residence time 2.0 s; (b) propane-lean feed: inlet composition 6.7 mol.% propane, 7% ammonia, 18% oxygen, remainder helium; residence time 2.0 s.

The reactor outlet was kept at 170 °C. On-line sampling of a volume of either the inlet or the outlet stream was obtained by means of three heated valves. Three different columns were used for the identification of products: (a) A Hay-sep T column (TCD detector) for the separation of CO_2, NH_3, $C_3H_8 + C_3H_6$, H_2O, HCN, acrolein, acetonitrile and acrylonitrile; Hay-sep T was also used as a filter to avoid the contamination of MS-5A by CO_2; (b) A MS-5A column (TCD detector) for the separation of O_2, N_2 and CO; and (c) A Poropak QS (FID detector) column for the separation of propane from propylene.

3. Results and discussion

3.1. Characterization of catalysts

Table 1 reports the theoretical atomic composition of samples, calculated on the basis of the amount of each precursor used for the preparation, the corresponding experimental composition for a few of them (as determined by X-ray Fluorescence) and the values of specific surface area. Samples prepared had Sn/V/Nb/Sb atomic ratios between components equal to $1/x/1/3$ ($0.2 \leq x \leq 0.8$). The XRF analysis was in good agreement with the theoretical compositions.

The surface area of samples was remarkably higher than that one typically reported for rutile-type mixed oxides prepared with conventional methodologies like the slurry-redox method, leading to areas systematically lower than 10 m^2/g. The increase of the V content led to a decrease of the surface area; this corresponds to an increase of the crystallinity of samples, as inferred from the X-ray diffraction patterns (see below).

The XRD patterns of calcined Sn/V/Nb/Sb $1/x/1/3$ samples are reported in Fig. 1. All patterns show the reflections of rutile SnO_2 cassiterite (JCPDS 005–0467). The increase of the V content led to a considerable enhancement of the crystallinity. This can be attributed to the incorporation of a part of Sb^{5+} and of Nb^{5+} cations into the Sn oxide lattice [14], in the sample with the lower V content ($x = 0.2$), with generation of defective, non-stoichiometric $Sn(Sb,Nb)O_2$, because of the charge unbalance created by the high-valent guest cations. However, the increase of the V content ($x > 0.2$) caused the preferential formation of a rutile V/Nb/Sb mixed oxide and to the generation of a less defective SnO_2, because of the lower amount of Sb and Nb incorporated in it. Therefore, one key-point for the development of a high surface area rutile-type mixed oxide is the formation of a defective, poorly crystalline material.

In samples with $x = 0.6$ and 0.8, weak reflections attributable to crystalline α-Sb_2O_4 were observed; this is a further proof of the expulsion of Sb from the tin oxide lattice and of its segregation into a separate oxide in more crystalline systems. However, a

Table 1
Theoretical and experimental bulk (X-ray fluorescence) atomic composition, and specific surface area of catalysts prepared

Theoretical composition (atomic ratios)	Experimental composition (atomic ratios)	Specific surface area (m^2/g)
Sn/V/Nb/Sb 1/0.2/1/3	1.00/0.20/1.16/2.81	74
Sn/V/Nb/Sb 1/0.4/1/3	nd	42
Sn/V/Nb/Sb 1/0.6/1/3	nd	33
Sn/V/Nb/Sb 1/0.8/1/3	1.00/0.61/1.05/3.44	23

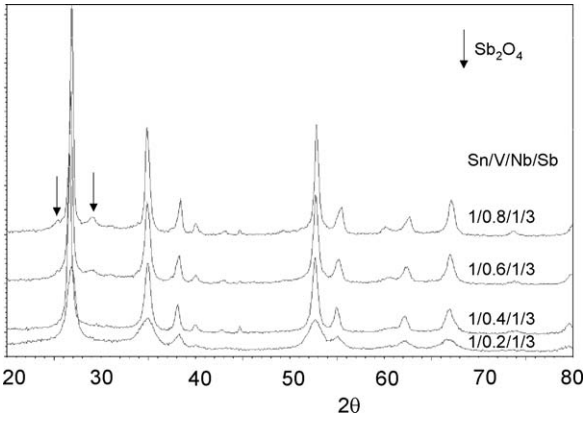

Fig. 1. X-ray diffraction patterns of calcined Sn/V/Nb/Sb $1/x/1/3$ catalysts.

preferential interaction of V with Nb [15], leading to the formation of a V/Nb mixed oxide and to the segregation of antimony oxide into Sb_2O_4, cannot be excluded. No diffraction lines attributable to crystalline vanadium oxide were observed, even for the highest V content.

Fig. 2 shows the Raman spectra of reference binary systems (Sn/Sb 1/1, Sb/Nb 1/1 and Sn/Nb 1/0.5) prepared with same co-precipitation method adopted for the multicomponent Sn/V/Nb/Sb systems. It is worth noting that SnO_2, also prepared with the same precipitation procedure, has a strong Raman band at 625–630 cm^{-1} and weaker ones at 770 and 685 cm^{-1}, all corresponding to bulk vibration modes [16,17]. The Raman spectrum of hydrated Nb oxide, after calcination at temperatures between 500 and 700 °C, shows a broad band at 680–690 cm^{-1} and less intense bands at 140, 220 and 310 cm^{-1}. From literature, the spectrum of $SbNbO_4$ shows bands at 845, 685, 620 and 380 cm^{-1} [18,19]. Our Sb/Nb 1/1 sample shows a strong band at 690 cm^{-1}, and less intense bands at 470, 410, 310, 230 and 130 cm^{-1}. The spectrum of Sn/Sb 1/1 shows differences with respect to that of SnO_2; in fact, the most intense band typical of tin oxide shifted from 630 to 640 cm^{-1}. This was likely due to the incorporation of Sb^{5+} into SnO_2 [20]. The band at 445 cm^{-1} is attributable to Sb_6O_{13}; however, the 100% intensity band of Sb_6O_{13} should fall at 470 cm^{-1}. This relevant shift can be attributed to the dissolution of guest cations, e.g., Sn^{4+} ions, inside the Sb oxide lattice. The broad band centred at around 830 cm^{-1} is attributable to cationic vacancies in rutile SnO_2, generated because of the incorporation of highly-valent Sb^{5+} cations, and specifically to the vibration of O–Sn(Sb) bond involving two-coordinated oxygen atoms adjacent to cationic vacancies [9,21]. A similar phenomenon was also evident

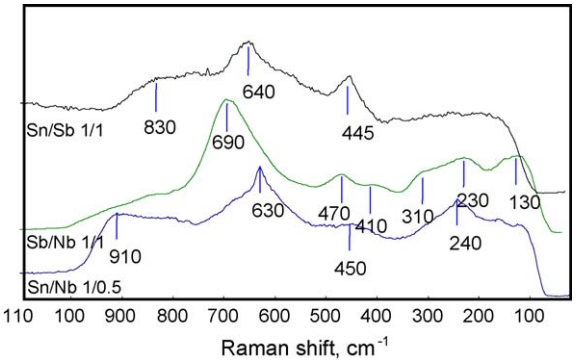

Fig. 2. Raman spectra of calcined bi-component reference samples: Sn/Sb 1/1, Sb/Nb 1/1 and Sn/Nb 1/0.5, recorded at ambient conditions.

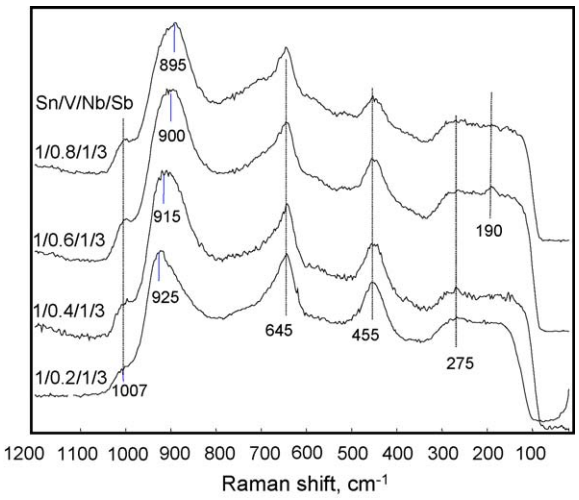

Fig. 3. Raman spectra of calcined Sn/V/Nb/Sb 1/*x*/1/3 catalysts, recorded at ambient conditions.

for the Sn/Nb 1/0.5 sample; in this case, the band attributable to the presence of O atoms neighbouring a cationic vacancy was centred at 910 cm^{-1}. In this sample, the most intense band associated to Sb_6O_{13} was observed at 450 cm^{-1}. These results indicate that the co-precipitation method adopted for the preparation of our samples led to the reciprocal dissolution of cations inside metal oxides, and to the generation of defective mixed oxides.

Raman spectra of calcined samples Sn/V/Nb/Sb 1/*x*/1/3 are reported in Fig. 3. Some bands were similar to those already observed in binary oxides; this is an evidence for the presence of Sn-containing Sb_6O_{13} and of Sb/Nb-containing SnO_2. A very intense band was observed at around 900 cm^{-1}, which however, shifted progressively from 925 to 895 cm^{-1} when the content of V was increased. Antimony was in large excess with respect to the amount required for the formation of the V/Nb/Sb mixed oxide; therefore the band attributed to the Sn-containing Sb oxide was not much affected by the addition of V. A very weak band at 190 cm^{-1} in the Sn/V/Nb/Sb 1/0.6/1/3 sample can be attributed to α-Sb_2O_4 that confirms the attribution of the weak reflections in the corresponding XRD pattern. However, this band is not observed in sample Sn/VNb/Sb 1/0.8/1/3, that contrasts with the evidence for the presence of α-Sb_2O_4 reflections in the XRD pattern (Fig. 1). One possible explanation for this incongruence is the development of Sb_2O_4 crystalline domains in the core of rutile crystals, that prevents it from being detected by Raman spectroscopy, a technique that is more suited for the characterization of the surface of samples.

On the other hand, Raman spectroscopy evidences the formation of amorphous Sb_6O_{13}, that contrasts with the usual formation of Sb_2O_4 and Sb_2O_3 in rutile-type V/Sb mixed oxides containing excess Sb. The formation of Sb_6O_{13} at the surface of rutile was already recorded for other rutile-type mixed oxides, e.g., in Cr/V/Nb/Sb/O [22], and is typically observed with samples prepared with the co-precipitation technique and calcined at 700 °C.

It is worth noting that the Raman features of vanadium oxide were not present, even in the sample having the highest V content ($x = 0.8$). This indicates that V was totally incorporated in the rutile-type V/Nb/Sb mixed oxide, and did not form extra-framework bulk species. The only band attributable to a VOx vibration was that one at 1005–1010 cm^{-1}; the intensity of this band slightly increased when the content of V was increased. It can be attributed to the stretching vibration of a V^{4+}=O species in rutile. In fact, isolated V species on supports, e.g., on titania or alumina, are characterized by a Raman band falling at wavenumber higher than 1015 cm^{-1} [23].

The strong band at around 900 cm^{-1} (the exact position being a function of the V content in samples), might be attributed to the vibration of V–O–V bond in oligomeric species dispersed at the catalyst surface [23], as in monolayer vanadium oxide over supports. However, the band of dispersed oligomeric VOx species is usually very broad and of very low intensity in supported vanadium oxide, if compared to bands attributable to the vibration modes of isolated and bulk vanadium oxide. Moreover, if this band were related to any V species dispersed on the rutile surface, its intensity should increase when the V content in samples is increased. Since this was not the case, we prefer to attribute the band at around 900 cm^{-1} to the Me–O vibration involving O ions adjacent to cationic vacancies in the rutile-type mixed oxide. In further support of this attribution, a strong band at around 900 cm^{-1} was also observed in the spectrum of rutile oxides that did not contain V at all [14], (see for instance the spectrum of sample Sn/Nb in Fig. 2).

Therefore, the presence of V led to the formation of a defective rutile-type V/Nb/Sb mixed oxide. The nature of defects was affected by the V content in catalysts, as evident from the progressive shift of the band at around 900 cm^{-1} towards lower wavenumber for increasing V content (Fig. 3); on the other hand, the latter only slightly affected the intensity of this band. Cationic vacancies in rutile oxides originate from the charge unbalance created by the dissolution of altervalent metal cations; for instance, in the case of the V/Nb/Sb mixed oxide, defects can derive from the Nb^{5+} cations replacing for V^{3+} and V^{4+}. On the other hand, increasing amounts of V in samples led to the decrease of the defectivity of SnO_2, because of the lower amount of guest cations incorporated in it. It can be hypothesized that an increase of the amount of the rutile-type V/Nb/Sb mixed oxide was compensated for by a lower density of vacancies, because of the lower amount of Nb^{5+}/Sb^{5+} replacing for $V^{3+/4+}$ in V/Nb/Sb/O and for Sn^{4+} in Sn(Sb,Nb)O_2. In fact, the increase of V content led to a better crystallinity of the rutile mixed oxides.

3.2. Catalytic performance in propane ammoxidation to acrylonitrile

Fig. 4 compares the catalytic performance of catalysts at propane-rich conditions. The conversion of propane (top) and the selectivity to acrylonitrile (middle) are shown in function of the reaction temperature. The bottom figure compares the selectivity to each reaction product obtained in correspondence of the highest selectivity to acrylonitrile. With all catalysts, the highest yield to acrylonitrile was obtained at total conversion of oxygen. With some catalysts, i.e., Sn/V/Nb/Sb 1/0.2/0.6/3 and 1/0.2/0.8/3, this also corresponds to the highest selectivity to acrylonitrile, whereas with catalysts having the lower amount of V, i.e., Sn/V/Nb/Sb 1/0.2/0.2/3 and 1/0.2/0.4/3, a decrease of the selectivity to acrylonitrile was shown when the temperature of total oxygen conversion was reached.

The increase of the V content in catalysts caused an increase of the catalytic activity. However, V had a detrimental effect on the maximum selectivity to acrylonitrile; the fall of the latter occurred with a corresponding increase of the selectivity to propene, CO and cyanhydric acid, and with an increase of ammonia combustion to N_2. The catalyst without V (Sn/V/Nb/Sb 1/0/1/3, not reported) showed very low activity; propane conversion was 4% at 520 °C, the selectivity to acrylonitrile being 48%.

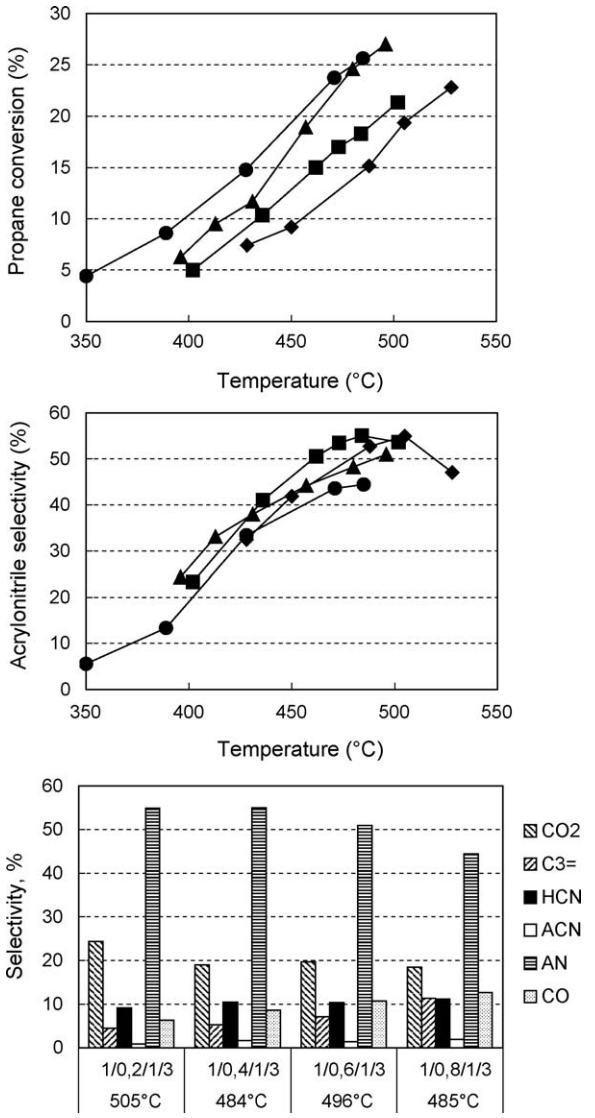

Fig. 4. Catalytic performance of Sn/V/Nb/Sb 1/*x*/1/3 catalysts at propane-rich conditions as a function of the reaction temperature. Top: propane conversion. Middle: selectivity to acrylonitrile. Bottom: selectivity to each reaction product at the temperature of maximum selectivity to acrylonitrile. Symbols: Sn/V/Nb/Sb 1/0.2/1/3 (◆), 1/0.4/1/3 (■), 1/0.6/1/3 (▲) and 1/0.8/1/3 (●).

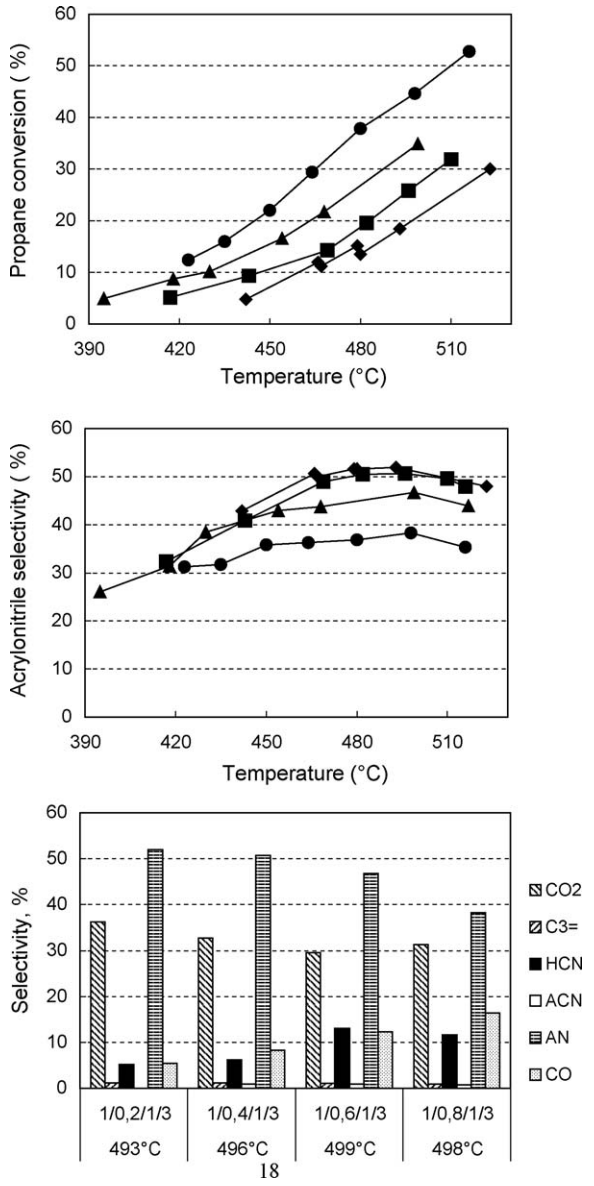

Fig. 5. Catalytic performance of Sn/V/Nb/Sb 1/*x*/1/3 catalysts at propane-lean conditions as a function of the reaction temperature. Top: propane conversion. Middle: selectivity to acrylonitrile. Bottom: selectivity to each reaction product at the temperature of maximum selectivity to acrylonitrile. Symbols: Sn/V/Nb/Sb 1/0.2/1/3 (◆), 1/0.4/1/3 (■), 1/0.6/1/3 (▲) and 1/0.8/1/3 (●).

With all catalysts, the increase of the reaction temperature led to higher selectivity to acrylonitrile and to a corresponding lower selectivity to propene, cyanhydric acid and acetonitrile. Cyanhydric acid was one major product at low temperature, especially with catalysts having the lower amount of V.

Fig. 5 compares the performance of catalysts at propane-lean conditions. With all samples, the selectivity to acrylonitrile was slightly lower than that achieved at propane-rich conditions, because of the higher formation of CO_2. This behavior is typically observed with all rutile-based catalysts for propane ammoxidation, which yield the best performance when high propane-to-oxygen feed ratios are used. Also in this case, the selectivity to acrylonitrile increased when the reaction temperature was raised; however, the variation of selectivity was less pronounced than that one experimentally observed at propane-rich conditions. Moreover, also in this case catalysts with the higher V content showed the lower maximum selectivity to acrylonitrile; however, differences between catalysts were more pronounced than at propane-rich conditions.

Fig. 5 (bottom) shows that the decrease of the maximum selectivity to acrylonitrile was due to a higher selectivity to cyanhydric acid and to CO. At high temperature, the selectivity to propene and to acetonitrile was very low for all catalysts investigated.

Fig. 6 compiles the specific rate of propane conversion in function of the V atomic fraction in catalysts, for both propane-rich and propane-lean conditions. The rates are referred either to the specific surface area of samples, or to the molar amount of V per unit catalyst weight in samples. The specific surface area decreased in proportion to the V atomic fraction in samples (Table 1). If a homogeneous reciprocal dispersion of the elements is assumed, a decrease of the rate referred to the V amount should be observed when the latter is increased. In fact, the fraction of exposed V sites, calculated with respect to the total V loading, is affected by the

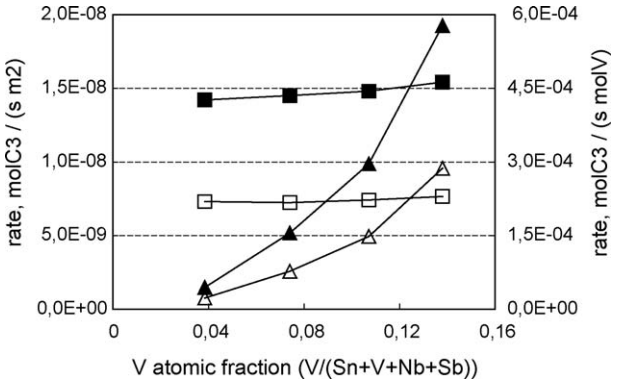

Fig. 6. Rate of propane conversion per unit mole of V loaded (■,□) and rate per unit surface area (▲,△), as functions of the V atomic content in catalysts, at propane-rich (T 400 °C, full symbols) and propane-lean (T 440 °C, open symbols) conditions.

surface area; in our samples, an increase of the amount of exposed V sites, due to the higher V loading, was compensated for by the decrease of surface area experimentally observed. On the other hand, the rate referred to the unit surface area should linearly increase, because of the higher surface density of exposed V sites occurring for an increase of the overall V loading.

On the contrary, Fig. 6 shows that the rate per unit surface area did not depend on the V atomic fraction, whereas the rate per mole of V increased exponentially. This indicates that the intrinsic activity of the V species, that one responsible for the activation of the alkane, improved when the V concentration in catalysts was increased.

In a previous work [14], we reported that a surface segregation of V, in the form of a rutile-type V/Sb/Nb mixed oxide, occurs in Sn/V/Nb/Sb 1/0.2/1/y samples having $y > 1$. A difference between the V atomic fraction at the surface and that in the bulk might lead to the experimental trends of Fig. 6, provided the surface segregation of V were more relevant in samples having the higher V content. However, the preferential surface segregation of V in V-richer samples would have led to Raman spectra in which the intensity of the band attributed to surface V=O species is remarkably increased with respect to that of samples having lower V content. Fig. 3 shows that indeed this was not the case. Therefore, the experimental trends shown in Fig. 6 can be explained by considering a role of the cationic vacancies [21,22,24]. A modification of the characteristics of vacancies, as shown by Raman spectroscopy, may be responsible for the enhancement of V activity in alkane conversion, and compensates for the increase of the rutile crystallinity and the decrease of the specific surface area.

4. Conclusions

Rutile-type Sn/V/Nb/Sb mixed oxides prepared by co-precipitation from an alcoholic medium are efficient catalysts for the ammoxidation of propane to acrylonitrile. Tin dioxide incorporates Sb^{5+} and Nb^{5+} cations, developing defective structures. The presence of increasing amounts of V in catalysts having composition Sn/V/Nb/Sb 1/x/1/3 (atomic ratios) considerably modified the chemical–physical and reactivity properties of samples, causing an increase of rutile crystallinity and a decrease of the specific surface area. Notwithstanding this, an enhancement of the activity of V species in the rutile-type V/Nb/Sb mixed oxide was experimentally observed, and was attributed to a change of the nature of cationic vacancies in rutile. On the other hand, the increase of activity led to catalysts less selective to acrylonitrile and more selective to propene and to undesired products, e.g., carbon monoxide and cyanhydric acid.

References

[1] P. Arpentinier, F. Cavani, F. Trifirò, The Technology of Catalytic Oxidations, Editions Technip, Paris, 2001.
[2] F. Cavani, F. Trifirò, Basic Principles in Applied Catalysis, in: Baerns M. (Ed.), Series in Chemical Physics, 75, Springer, Berlin, 2003, p. 21.
[3] R.K. Grasselli, Top. Catal. 21 (2002) 79.
[4] G. Centi, S. Perathoner, F. Trifirò, Appl. Catal. A 157 (1997) 143.
[5] Y. Moro-oka, W. Ueda, Royal Society of Chemistry 11 (1994) 223 (Catalysis).
[6] T. Ushikubo, K. Oshima, A. Kayou, M. Vaarkamp, M. Hatano, J. Catal. 169 (1997) 394.
[7] M. Florea, R. Prada Silvy, P. Grange, Appl. Catal. A 286 (2005) 1.
[8] M. Olea, M. Florea, I. Sack, R. Prada Silvy, E.M. Gaigneaux, G.B. Marin, P. Grange, J. Catal. 232 (2005) 152.
[9] J. Nilsson, A.R. Landa-Canovas, S. Hansen, A. Andersson, J. Catal. 186 (1999) 442.
[10] H. Roussel, B. Mehlomakulu, F. Belhadj, E. Van Steen, J.M.M. Millet, J. Catal. 205 (2002) 97.
[11] V.D. Sokolovskii, A.A. Davydov, O.Yu. Ovsitser, Catal. Rev. Sci. Eng. 37 (3) (1995) 425.
[12] S. Albonetti, G. Blanchard, P. Burattin, F. Cavani, F. Trifirò, US 6,083,869, assigned to Rhodia.
[13] S. Albonetti, G. Blanchard, P. Burattin, F. Cavani, S. Masetti, F. Trifirò, Catal. Today 42 (1998) 283.
[14] E. Arcozzi, N. Ballarini, F. Cavani, M. Cimini, C. Lucarelli, F. Trifirò, P. Delichere, J.-M.M. Millet, P. Marion, Catal. Today 138 (2008) 97.
[15] M.O. Guerrero-Perez, J.L.G. Fierro, M.A. Bañares, Catal. Today 118 (2006) 366.
[16] J.M. Herrmann, F. Villain, L.G. Appel, Appl. Catal. A 240 (2003) 177.
[17] S. Loridant, J. Phys. Chem. B 106 (2002) 13273.
[18] M.O. Guerrero-Perez, J.L.G. Fierro, M.A. Bañares, Catal. Today 78 (2003) 387.
[19] M.O. Guerrero-Perez, J.L.G. Fierro, M.A. Bañares, Phys. Chem. Chem. Phys. 5 (2003) 4032.
[20] M. Caldararu, M.F. Thomas, J. Bland, D. Spranceana, Appl. Catal. A 209 (2001) 383.
[21] M. Cimini, J.M.M. Millet, F. Cavani, J. Solid State Chem. 177 (2004) 1045.
[22] N. Ballarini, F. Cavani, M. Cimini, F. Trifirò, J.M.M. Millet, U. Corsaro, R. Catani, J. Catal. 241 (2006) 255.
[23] M.A. Banares, I.E. Wachs, J. Raman Spectr. 33 (2002) 359.
[24] G. Xiong, V.S. Sullivan, P.C. Stair, G.W. Zajac, S.S. Trail, J.A. Kaduk, J.T. Golab, J.F. Brazdil, J. Catal. 230 (2005) 317.